

An Optimized Path Planning of Manipulator Using Spline Curves and Real Quantifier Elimination Based on Comprehensive Gröbner Systems

Yusuke Shirato¹, Natsumi Oka¹, Akira Terui^{2*}, Masahiko Mikawa³

¹ Graduate School of Pure and Applied Sciences, University of Tsukuba,
Tsukuba-shi, 305-8571, Ibaraki, Japan.

^{2*} Faculty of Pure and Applied Sciences, University of Tsukuba,
Tsukuba-shi, 305-8571, Ibaraki, Japan.

³ Faculty of Library, Information and Media Science, University of
Tsukuba, Tsukuba-shi, 305-8550, Ibaraki, Japan.

*Corresponding author(s). E-mail(s): terui@math.tsukuba.ac.jp;
Contributing authors: mikawa@slis.tsukuba.ac.jp;

Abstract

This paper presents an advanced method for addressing the inverse kinematics and optimal path planning challenges in robot manipulators. The inverse kinematics problem involves determining the joint angles for a given position and orientation of the end-effector. Furthermore, the path planning problem seeks a trajectory between two points. Traditional approaches in computer algebra have utilized Gröbner basis computations to solve these problems, offering a global solution but at a high computational cost. To overcome the issue, the present authors have proposed a novel approach that employs the Comprehensive Gröbner System (CGS) and CGS-based quantifier elimination (CGS-QE) methods to efficiently solve the inverse kinematics problem and certify the existence of solutions for trajectory planning. This paper extends these methods by incorporating smooth curves via cubic spline interpolation for path planning and optimizing joint configurations using shortest path algorithms to minimize the sum of joint configurations along a trajectory. This approach significantly enhances the manipulator's ability to navigate complex paths and optimize movement sequences.

Keywords: Comprehensive Gröbner Systems, Quantifier elimination, Robotics, Inverse kinematics, Spline interpolation, Shortest path algorithms

MSC Classification: 68W30 , 13P10 , 13P25 , 68U07 , 68R10

1 Introduction

This paper discusses a method for solving the inverse kinematics problem and the optimal path planning problem for a robot manipulator. A manipulator is a robot with links corresponding to human arms and joints corresponding to human joints, and the tip is called the end-effector. The inverse kinematics problem for manipulators is to find the angle of each joint, given the position and orientation of the end-effector. The path planning problem is to find a path to move the end-effector between two specified positions [1].

When operating the manipulator, one needs to solve the inverse kinematics problem (or the path planning problem, respectively) for the desired end-effector position (or the series of positions, respectively).

Methods of solving inverse kinematics problems for manipulators by reducing the inverse kinematics problem to a system of polynomial equations and using the Gröbner basis has been proposed [2–6]. Solving the inverse kinematics problem using the Gröbner basis computation has an advantage that the global solution of the inverse kinematics problem can be obtained before the end-effector will actually be “moved” by simulation or other means. On the other hand, the Gröbner basis computation has the disadvantage of relatively high computational cost compared to local solution methods such as the Newton method. Furthermore, when solving a path planning problem using the Gröbner basis computation, it is necessary to solve the inverse kinematics problem for each point on the path, which is even more computationally expensive.

The third and fourth authors have also previously proposed methods for solving inverse kinematics problems using Gröbner basis computations [7–9]. The authors’ contributions in their previous work [9] are as follows. We have proposed a method for solving the inverse kinematics problem and the trajectory planning problem of a 3 Degree-Of-Freedom (DOF) manipulator using the Comprehensive Gröbner System (CGS) [10]. In the proposed method, the inverse kinematic problem has been expressed as a system of polynomial equations with the coordinates of the end-effector as parameters and the CGS is calculated in advance to reduce the cost of Gröbner basis computation for each point on the path. In addition, we have proposed a method for solving the inverse kinematics problems using the CGS-QE method [11], which is a quantifier elimination (QE) method based on CGS computations, to certify the existence of a (real) solution. Furthermore, we have proposed a method to certify the existence of a solution to the whole trajectory planning problem using the CGS-QE method, where the points on the trajectory are represented by parameters.

This paper proposes the following method as an extension of the previous work [9].

1. Extension of paths used in path planning problems: while the previous work has used straight lines, this paper uses smooth curves generated by the cubic spline interpolation passing through given points. For example, a curved path allows us to plan paths that avoid obstacles.
2. Optimization of the joint configuration obtained as the solution to the path planning problem: when solving the path planning problem, there can be multiple solutions to the inverse kinematics problem at each point on the path. In this case, the question is which of the solutions for adjacent points can be connected to minimize the sum of the configurations of the entire sequence of the joints. In this paper, we reduce this problem to the shortest path problem of a weighted graph and propose a method to compute the optimal sequence of joint configurations using shortest path algorithms.

This paper is organized as follows. In Section 2, we describe the inverse kinematics problem for a 3-DOF manipulator and the method of solving it. In Section 3, the method of generating trajectories using cubic spline interpolation is proposed. In Section 4, we describe the method of optimizing the joint configuration obtained as the solution to the path planning problem. In Section 5, we give concluding remarks and future research directions.

2 Solving the inverse kinematic problem

The manipulator used in this paper is myCobot 280 [12] from Elephant Robotics, Inc. (hereafter referred to simply as “myCobot”). Although myCobot is a 6-DOF manipulator, we treat it as a 3-DOF manipulator by operating only the three main joints used to move the end-effector while the remaining joints are fixed.

The forward kinematics problem for myCobot is derived using the modified Denavit-Hatenberg convention (hereafter abbreviated as “D-H convention”), which is standard in robotics [1]. Each link is sequentially named Link 0, Link 1, \dots , and Link 7, starting from a fixed point to the end effector. For $i = 1, 2, \dots, 7$, the joint connecting Link $(i - 1)$ and Link i is called Joint i . Additionally, the endpoint of Link 0 that is not connected to Joint 1 is called Joint 0, and the end effector is called Joint 8. The 3D right-handed coordinate system at joint i ($i = 0, 1, \dots, 8$) is denoted by Σ_i . The origin of Σ_1 is Joint 2, and for $i \neq 1$, the origin of Σ_i is Joint i . If Joint i is a rotational joint, let the z_i axis be its rotation axis. Other axes and their directions are set to make the transformation matrix from coordinate system Σ_i to coordinate system Σ_{i-1} relatively simple. Figure 1 shows the model of myCobot with the coordinates of each joint. In the representation of coordinate axes, the axis pointing from the back of the page to the front is shown as the “arrowhead,” while the axis pointing from the front of the page to the back is depicted as the “arrow tail” (a circle with a cross mark).

Next, we provide the transformation matrix between the coordinate systems of myCobot. To represent the relationship between adjacent coordinate systems, we define the parameters $a_i, \alpha_i, d_i, \theta_i$ for Σ_{i-1} and Σ_i as follows:

- a_i : The distance between the z_{i-1} axis and the z_i axis [mm],
- α_i : The angle from the z_{i-1} axis to the z_i axis around the x_{i-1} axis [rad],
- d_i : The distance between the x_{i-1} axis and the x_i axis [mm],

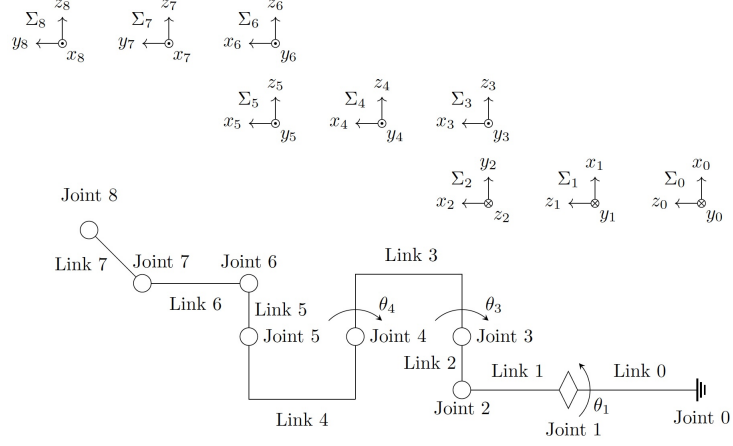


Fig. 1 The model of myCobot.

Table 1 Parameters of each joint.

i	a_i	α_i	d_i	θ_i
1	0	0	131.56	θ_1
2	0	$-\frac{\pi}{2}$	0	$-\frac{\pi}{2}$
3	0	$-\frac{\pi}{2}$	33.195	θ_3
4	110.4	0	0	θ_4
5	96.0	0	0	0
6	0	0	33.195	0
7	73.18	0	0	$-\frac{\pi}{2}$
8	43.6	0	0	0

- θ_i : The angle from the x_{i-1} axis to the x_i axis around the z_i axis [rad].

Table 1 shows the parameters of each joint. By using these parameters, the transformation matrix ${}^{i-1}T_i$ from Σ_i to Σ_{i-1} is given as

$$\begin{aligned}
{}^{i-1}T_i &= \begin{pmatrix} 1 & 0 & 0 & a_i \\ 0 & 1 & 0 & 0 \\ 0 & 0 & 1 & 0 \\ 0 & 0 & 0 & 1 \end{pmatrix} \begin{pmatrix} 1 & 0 & 0 & 0 \\ 0 & \cos \alpha_i & -\sin \alpha_i & 0 \\ 0 & \sin \alpha_i & \cos \alpha_i & 0 \\ 0 & 0 & 0 & 1 \end{pmatrix} \\
&\times \begin{pmatrix} 1 & 0 & 0 & 0 \\ 0 & 1 & 0 & 0 \\ 0 & 0 & 1 & d_i \\ 0 & 0 & 0 & 1 \end{pmatrix} \begin{pmatrix} \cos \theta_i & -\sin \theta_i & 0 & 0 \\ \sin \theta_i & \cos \theta_i & 0 & 0 \\ 0 & 0 & 1 & 0 \\ 0 & 0 & 0 & 1 \end{pmatrix} \\
&= \begin{pmatrix} \cos \theta_i & -\sin \theta_i & 0 & a_i \\ \cos \alpha_i \sin \theta_i & \cos \alpha_i \cos \theta_i & -\sin \alpha_i & -d_i \sin \alpha_i \\ \sin \alpha_i \sin \theta_i & \sin \alpha_i \cos \theta_i & \cos \alpha_i & d_i \cos \alpha_i \\ 0 & 0 & 0 & 1 \end{pmatrix}, \tag{1}
\end{aligned}$$

where the affine coordinates are used to represent the transformation matrix.

Let the coordinates of the end effector in the Σ_0 coordinate system be (x, y, z) , and the transformation matrix from the Σ_8 coordinate system to the Σ_0 coordinate system be $T = {}^0T_1{}^1T_2{}^2T_3{}^3T_4{}^4T_5{}^5T_6{}^6T_7{}^7T_8$. Since the end effector is located at the origin of the Σ_8 coordinate system, the coordinates of the end effector in the Σ_0 coordinate system can be expressed as

$$\begin{pmatrix} x \\ y \\ z \\ 1 \end{pmatrix} = T \begin{pmatrix} 0 \\ 0 \\ 0 \\ 1 \end{pmatrix}. \quad (2)$$

By expressing $s_i = \sin \theta_i$ and $c_i = \cos \theta_i$ for $i = 1, 3, 4$, eq. (2) can be rewritten as

$$\begin{aligned} -169.18s_1s_3c_4 - 169.18s_1c_3s_4 - 43.6s_1s_3s_4 + 43.6s_1c_3c_4 \\ -110.4s_1s_3 - 66.39c_1 + x &= 0, \\ 169.18c_1s_3c_4 + 169.18c_1c_3s_4 + 43.6c_1s_3s_4 - 43.6c_1c_3c_4 \\ +110.4c_1s_3 - 66.39s_1 + y &= 0, \\ -169.18c_3c_4 + 169.18s_3s_4 - 43.6c_3s_4 - 43.6s_3c_4 \\ -110.4c_3 - 131.56 + z &= 0, \\ s_1^2 + c_1^2 - 1 = 0, \quad s_3^2 + c_3^2 - 1 = 0, \quad s_4^2 + c_4^2 - 1 = 0. \end{aligned} \quad (3)$$

In the following, for a set of polynomials $F = \{f_1, \dots, f_m\} \subset \mathbb{R}[c_1, s_1, c_3, s_3, c_4, s_4]$, The system of polynomial equations $f_1 = \dots = f_m = 0$ is denoted by $F = 0$. Since the first, second, and third equations of eq. (3) contain decimal coefficients, both sides of these equations are actually multiplied by 100. Thus, we obtain the inverse kinematic problem as the one to find the solution $c_1, s_1, c_3, s_3, c_4, s_4$ to the system of polynomial equations $F = 0$ with $F = \{f_1, \dots, f_6\}$, where

$$\begin{aligned} f_1 &= -16918s_1s_3c_4 - 16918s_1c_3s_4 - 4360s_1s_3s_4 + 4360s_1c_3c_4 - 11040s_1s_3 \\ &\quad - 6639c_1 + 100x, \\ f_2 &= 16918c_1s_3c_4 + 16918c_1c_3s_4 + 4360c_1s_3s_4 - 4360c_1c_3c_4 + 11040c_1s_3 \\ &\quad - 6639s_1 + 100y, \\ f_3 &= -16918c_3c_4 + 16918s_3s_4 - 4360c_3s_4 - 4360s_3c_4 - 11040c_3 \\ &\quad - 13156 + 100z, \\ f_4 &= s_1^2 + c_1^2 - 1, \quad f_5 = s_3^2 + c_3^2 - 1, \quad f_6 = s_4^2 + c_4^2 - 1. \end{aligned} \quad (4)$$

Note that the system of equations $F = 0$ has parameters x, y, z in the coefficients.

The inverse kinematic problem is solved as follows. With our previously proposed method [9, Algorithm 1], before solving $F = 0$, we calculate the CGS of $\langle f_1, \dots, f_6 \rangle$. Then, for a given end-effector coordinate $(x, y, z) = (\alpha, \beta, \gamma) \in \mathbb{R}^3$, determine the feasibility of such a configuration using the CGS-QE method. If the configuration is feasible, we solve $F = 0$ numerically after substituting parameters x, y, z with α, β, γ , respectively, to obtain the inverse kinematic solution.

3 Path and trajectory planning using spline interpolation

In the path planning problem, a finite number of points through which the path passes are given in advance, and a trajectory is generated on the smooth path passing through these points. While a straight line was used as the path in our previous study, a path is generated using cubic spline interpolation [13] in the present paper.

3.1 Path planning using cubic spline interpolation

Let (x_0, y_0, z_0) , (x_1, y_1, z_1) , (x_2, y_2, z_2) , (x_3, y_3, z_3) be four different points given in \mathbb{R}^3 . For $j = 0, 1, 2$, calculate a curve C_j passing through (x_j, y_j, z_j) and $(x_{j+1}, y_{j+1}, z_{j+1})$ in the form of a function $(X_j(s), Y_j(s), Z_j(s))$ with $s \in [0, 1]$ as a parameter. In cubic spline interpolation, $X_j(s), Y_j(s), Z_j(s)$ are cubic polynomials given by

$$\begin{aligned} X_j(s) &= a_{X,j}s^3 + b_{X,j}s^2 + c_{X,j}s + d_{X,j}, \\ Y_j(s) &= a_{Y,j}s^3 + b_{Y,j}s^2 + c_{Y,j}s + d_{Y,j}, \\ Z_j(s) &= a_{Z,j}s^3 + b_{Z,j}s^2 + c_{Z,j}s + d_{Z,j}, \end{aligned} \quad (5)$$

where $a_{X,j}, b_{X,j}, \dots, d_{Z,j}$ are real numbers. Furthermore, we impose the following conditions on these functions.

$$\begin{aligned} (X_j(j), Y_j(j), Z_j(j)) &= (x_j, y_j, z_j), \quad j = 0, 1, 2, \\ (X_j(j+1), Y_j(j+1), Z_j(j+1)) & \\ &= (x_{j+1}, y_{j+1}, z_{j+1}), \quad j = 0, 1, 2, \\ (X'_j(j+1), Y'_j(j+1), Z'_j(j+1)) & \\ &= (X'_{j+1}(j+1), Y'_{j+1}(j+1), Z'_{j+1}(j+1)), \quad j = 0, 1, \\ (X''_j(j+1), Y''_j(j+1), Z''_j(j+1)) & \\ &= (X''_{j+1}(j+1), Y''_{j+1}(j+1), Z''_{j+1}(j+1)), \quad j = 0, 1. \end{aligned} \quad (6)$$

In this paper, in addition to the conditions in eq. (6), we find the *natural* cubic Spline interpolation that satisfies

$$X''_0(0) = X''_3(3) = Y''_0(0) = Y''_3(3) = Z''_0(0) = Z''_3(3) = 0. \quad (7)$$

The coefficients of $X_j(s)$ are determined as follows (the coefficients of $Y_j(s)$ and $Z_j(s)$ are determined similarly). In general, suppose that N points $(x_0, y_0), \dots, (x_N, y_N)$ are given, and, for $j = 0, \dots, N-1$, the curve C_j passing through (x_j, y_j, z_j) and $(x_{j+1}, y_{j+1}, z_{j+1})$ are to be calculated. Let $v_{x,j+1} = 6(x_j - 2x_{j+1} + x_{j+2})$ for $j = 0, \dots, N-2$ and $v_{x,0} = v_{x,N-1} = 0$. Then, define $u_{X,j}$ as the solution to the

following system of linear equations:

$$\begin{pmatrix} 4 & 1 & & & \\ 1 & 4 & 1 & & \\ & \ddots & \ddots & \ddots & \\ & & & 1 & 4 & 1 \\ & & & & 1 & 4 \end{pmatrix} \begin{pmatrix} u_{X,1} \\ u_{X,2} \\ \vdots \\ u_{X,N-2} \\ u_{X,N-1} \end{pmatrix} = \begin{pmatrix} v_{x,1} \\ v_{x,2} \\ \vdots \\ v_{x,N-2} \\ v_{x,N-1} \end{pmatrix}. \quad (8)$$

Furthermore, set $u_{X,0} = u_{X,N} = 0$ by the natural spline condition (eq. (7)). Then, the coefficients $a_{X,j}, b_{X,j}, c_{X,j}, d_{X,j}$ of $X_j(s)$ are determined as

$$\begin{aligned} a_{X,j} &= \frac{1}{6}(u_{X,j+1} - u_{X,j}), & b_{X,j} &= \frac{u_{X,j}}{2}, \\ c_{X,j} &= x_{j+1} - x_j - \frac{1}{6}(u_{X,j+1} + 2u_{X,j}), & d_{X,j} &= x_j, \end{aligned}$$

for $j = 0, \dots, N-1$.

3.2 Solving the inverse kinematics problem

We generate the trajectory for the curve C_j obtained in the previous section by solving the inverse kinematics problem using the following procedure.

First, using the CGS-QE method, we determine the existence of solutions to the inverse kinematics problem for each curve C_j ($j = 0, 1, 2$) that constitutes the path to move the end-effector. In eq. (4), replace x, y, z in each equation by $X_j(s), Y_j(s), Z_j(s)$, respectively, to obtain a system of polynomial equations with s as parameter. Let the result be $\bar{F}_j(s)$.

Next, we apply the CGS-QE method to $\bar{F}_j(s)$ to determine whether the system of equations $\bar{F}_j(s) = 0$ has real solutions within the parameter $s \in [0, 1]$. If $\bar{F}_j(s) = 0$ has real solutions within the parameter $s \in [0, 1]$, we calculate the trajectory of the end-effector's position by changing s with a series of time steps $t = 0, \dots, T$, where T is a positive integer. For time $t = 0, \dots, T$, let $s = f(t)$ where f is a continuous function of $[0, T] \rightarrow [0, 1]$. To ensure that the end-effector has no velocity and acceleration at the beginning and end of the trajectory, we obtain f as a polynomial of the smallest degree possible to satisfy $f'(t) = f''(t) = 0$ at $t = 0$ and T . Then, we obtain

$$f(t) = \left(\frac{6t^5}{T^5} - \frac{15t^4}{T^4} + \frac{10t^3}{T^3} \right) \quad (9)$$

(see [9, 14]).

Finally, For $j = 0, 1, 2$ and $t = 0, \dots, T$, the configuration of the joints is obtained by solving the system of polynomial equations

$$\bar{F}_j(f(t)) = 0. \quad (10)$$

Algorithm 1 Path and trajectory planning with spline interpolation

Input: The points that the end-effector of myCobot should pass through, including the initial position and the target position: $(x_0, y_0, z_0), \dots, (x_N, y_N, z_N)$, The number of time steps: T

Output: A set of the tuple $(\theta_1, \theta_3, \theta_4)$ for each of the $(N \times T + 1)$ points on the spline curve passing through the input points

```
1:  $A \leftarrow \emptyset$ ;
2: Solve the inverse kinematic problem eq. (4) for  $(x, y, z) = (x_0, y_0, z_0)$  with the
   algorithm for the inverse kinematics problem [9, Algorithm 1];
3: if no solution is obtained then
4:   return Error;
5: end if
6:  $A \leftarrow A \cup \{(\theta_1, \theta_3, \theta_4)\}$ ;
7: For  $(x_0, y_0, z_0), \dots, (x_N, y_N, z_N)$ , input to the algorithm for spline interpolation
   [13] to obtain the spline curve  $(X_j(s), Y_j(s), Z_j(s))$ ;
8: for  $j \in [0, \dots, N - 1]$  do
9:   Put  $f(t)$  in eq. (9) into  $s$  in  $(X_j(s), Y_j(s), Z_j(s))$ ;
10:  for  $t \in [1, \dots, T]$  do
11:    Solve the inverse kinematic problem eq. (10) for  $(X_j(t), Y_j(t), Z_j(t))$  with
    the algorithm for the inverse kinematics problem [9, Algorithm 1];
12:    if no solution is obtained then
13:      return Error,  $(j, t)$ ;
14:    else
15:       $A \leftarrow A \cup \{(\theta_1, \theta_3, \theta_4)\}$ ;
16:    end if
17:  end for
18: end for
```

3.3 An algorithm for path and trajectory planning with spline interpolation

Summarizing the above, an algorithm for path and trajectory planning with spline interpolation is given in Algorithm 1.

3.4 Implementation and computational results

This section describes the implementation and experimental results of the proposed method. We implemented Algorithm 1 on the computer algebra system Risa/Asir [15] and used it together with our existing implementation of inverse kinematics calculations [9]. For the CGS calculation, we used an algorithm by Kapur et al. [16] with an implementation by Nabeshima [17]. The existence of the root of the inverse kinematics problem by the CGS-QE method was verified using Risa/Asir with accompanying Wolfram Mathematica 13.1 [18] for simplifying the expression.

We measured the computation time for the path and the trajectory planning of myCobot for each of the six types of input points (x_0, y_0, z_0) , (x_1, y_1, z_1) , (x_2, y_2, z_2) , (x_3, y_3, z_3) , as below, for $T = 10$ and $T = 50$.

Table 2 Computation time for path and trajectory planning of myCobot.

Test	$T = 10$ [s]	$T = 50$ [s]
1	1.293	7.836
2	1.342	6.490
3	1.296	8.049
4	1.574	7.616
5	1.265	7.155
6	Fail	Fail
Average	1.354	7.429

Test 1 $(-100, -100, 100), (0, -150, 50), (50, -100, 50), (100, 0, 0),$
Test 2 $(-150, -100, 150), (0, -100, 100), (100, -50, 50), (100, 100, 0),$
Test 3 $(-250, 0, 0), (-150, 0, 50), (-150, 100, 150), (250, 100, 100),$
Test 4 $(100, 50, 0), (50, 100, 150), (-150, 150, 100), (-150, 50, 50),$
Test 5 $(100, 100, -50), (50, 100, 0), (-100, 100, 50), (-150, -50, 100),$
Test 6 $(150, 150, 0), (50, 50, 100), (-50, -50, 100), (-150, -150, 50).$

The computing environment is as follows: Intel Xeon Silver 4210 3.2 GHz, RAM 256 GB, Linux Kernel 5.4.0, Risa/Asir Version 20230315.

Table 2 shows the result of the experiment. The CGS of the ideal generated by the polynomials in eq. (4) used in the experiment was calculated in advance¹. The columns “ $T = 10$ ” and “ $T = 50$ ” show each test’s computation time with $T = 10$ and 50, respectively. The data labeled “Fail” means that during the computation, it was discovered that part of the generated spline does not lie within the feasible region of myCobot for the given sequence of points, and thus, the computation was aborted. The computation results suggest that the computation time is approximately linearly proportional to T . Additionally, it indicates that the curve designed with the spline may exceed the feasible region of myCobot, and measures are needed to address such cases.

4 Choosing an optimal path from multiple solutions of inverse kinematics

When executing the trajectory planning of myCobot, as shown in the previous section, the inverse kinematics problem eq. (4) may have multiple solutions at each time t . When actually operating the manipulator, it is necessary to select one solution uniquely. Therefore, in this section, we propose and examine two methods for deriving the optimal path for the manipulator’s operation.

As a preparation, first, let the points where the end effector moves be p_1 (starting point), p_2, \dots, p_{n-1}, p_n (ending point). The points p_1, \dots, p_n divide the curve (derived with the proposed method) into $n - 1$ equal segments when the end effector passes through. In the previous section on path and trajectory planning, we observed four solutions to the inverse kinematics problem at each point on the trajectory. This means that at each of p_1, \dots, p_n , there are four possible configurations of the joints,

¹The CGS was calculated in approximately 0.16 [s] on the following computing environment: Intel Celeron J4125 2.00 GHz, RAM 5.6 GB, Ubuntu 22.04.3 LTS, Risa/Asir: version 20230315.

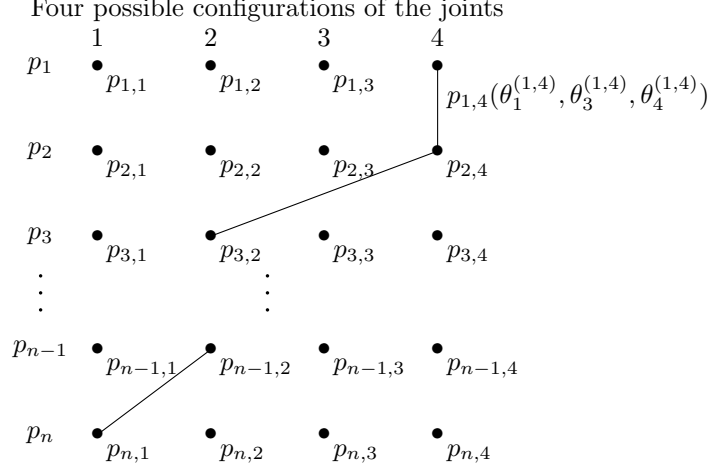


Fig. 2 Four possible configurations of the joints at each point on the path.

which we denote as $p_{1,1}, p_{1,2}, \dots, p_{1,4}, \dots, p_{n,1}, p_{n,2}, \dots, p_{n,4}$. In other words, $p_{i,j}$ ($i = 1, \dots, n, j = 1, 2, 3, 4$) refers to the j -th possible configuration of the joints at point p_i . Additionally, since each $p_{i,j}$ has values for θ_1, θ_3 , and θ_4 (in units of [rad]) as its elements, we denote them as $p_{i,j} = (\theta_1^{(i,j)}, \theta_3^{(i,j)}, \theta_4^{(i,j)})$ (see fig. 2).

Next, we define the magnitude of the joint variations between each point. When the end effector moves from point and configuration (hereafter simply referred to as “point”) $p_{i,j}$ to point $p_{i+1,k}$ ($k = 1, 2, 3, 4$), the magnitude of the joint variations is defined by

$$s_{i,j,i+1,k} = |\theta_1^{(i+1,k)} - \theta_1^{(i,j)}| + |\theta_3^{(i+1,k)} - \theta_3^{(i,j)}| + |\theta_4^{(i+1,k)} - \theta_4^{(i,j)}|. \quad (11)$$

4.1 Minimizing the magnitude of joint variations between each point

The first method is trajectory planning that minimizes the magnitude of joint variations $s_{i,j,i+1,k}$ between each point. The following calculations are repeated for $m = 1, 2, 3, 4$.

Step 1. Calculate all $s_{1,m,2,k}$ from the starting point $p_{1,m}$ to the points $p_{2,k}$ ($k = 1, 2, 3, 4$), and select the point $p_{2,k}$ with the smallest $s_{1,m,2,k}$, denoting it as $p_{2,k'}$.

Step 2. From the point ($p_{2,k'}$) selected in item [Step 1.](#), calculate all $s_{2,k',3,k}$ to the points $p_{3,k}$, and select the point $p_{3,k}$ with the smallest $s_{2,k',3,k}$, denoting it as $p_{3,k'}$.

Step 3. Similarly, from the point ($p_{i,k'}$) selected in the previous step, calculate all $s_{i,k',i+1,k}$ to the next points ($p_{i+1,k}$), and select the point with the smallest $s_{i,k',i+1,k}$, denoting it as $p_{i+1,k'}$. Repeat this process until the endpoint $p_{n,k'}$ is determined.

Among the paths starting from these four initial points, the path that minimizes the sum of the magnitudes of the joint variations between the selected points, expressed as

$$S_{1,m,n,k'} = s_{1,m,2,k'} + \sum_{i=2}^{n-1} s_{i,k',i+1,k'},$$

will be the desired path for this section.

If each point on the trajectory has d possible configurations, the complexity of this method is $O(nd)$.

4.2 Minimizing the sum of the magnitudes of the joint variations from the starting point to the endpoint

The second method is trajectory planning, which minimizes the sum of the magnitudes of the joint variations between each point from the starting point to the endpoint.

For this purpose, we define a weighted graph $G = (V, E)$, where $V = \{p_{i,j} \mid i \in \{0, \dots, n\}, j \in \{1, \dots, d\}\}$ is the set of vertices corresponding to the joint configuration at each point and $E = \{(p_{i,j}, p_{i+1,k}) \mid i \in \{0, \dots, n-1\}, j, k \in \{0, \dots, d\}\}$ is the set of edges connecting the vertices at adjacent points. We estimate the shortest path from the starting point $p_{1,m}$ ($m = 1, 2, 3, 4$) to the endpoint $p_{n,k}$ in G using Dijkstra's algorithm [19] as follows, with the weight of the edge $(p_{i,j}, p_{i+1,k})$ defined as the the magnitude of the joint variations $s_{i,j,i+1,k}$ in eq. (11). As an initial setting, the shortest distance from the starting point to itself is set to 0, and the shortest distance to all other points is set to ∞ .

- Step 1. Set the beginning point to $p_{1,m}$. Set the shortest distance from the starting point to itself to 0 and the shortest distance to all other points to ∞ .
- Step 2. Move to the points $p_{2,1}, p_{2,2}, p_{2,3}, p_{2,4}$ which are adjacent to $p_{1,m}$, and compare the existing shortest distances (all ∞ for the four points) with the total travel distances to each point ($0 + s_{1,m,2,1} = s_{1,m,2,1}$, $0 + s_{1,m,2,2} = s_{1,m,2,2}$, $0 + s_{1,m,2,3} = s_{1,m,2,3}$, $0 + s_{1,m,2,4} = s_{1,m,2,4}$), and set the smallest values among $s_{1,m,2,1}, s_{1,m,2,2}, s_{1,m,2,3}, s_{1,m,2,4}$ as the new shortest distances from $p_{1,m}$ to $p_{2,1}, p_{2,2}, p_{2,3}, p_{2,4}$.
- Step 3. For $k = 1, 2, 3, 4$, repeat the following calculations: move to the points $p_{3,1}, p_{3,2}, p_{3,3}, p_{3,4}$ which are adjacent to $p_{2,k}$, compare the existing shortest distances with the total travel distances to each point

$$\begin{aligned} & s_{1,m,2,k} + s_{2,k,3,1}, \quad s_{1,m,2,k} + s_{2,k,3,2}, \\ & s_{1,m,2,k} + s_{2,k,3,3}, \quad s_{1,m,2,k} + s_{2,k,3,4}, \end{aligned} \tag{12}$$

and set the smallest values among eq. (12) as the new shortest distances from $p_{1,m}$ to $p_{3,1}, p_{3,2}, p_{3,3}$, and $p_{3,4}$.

- Step 4. Similarly, for $i = 3, \dots, n-1$ and $k = 1, 2, 3, 4$, move to the points $p_{i+1,1}, p_{i+1,2}, p_{i+1,3}, p_{i+1,4}$ which are adjacent to $p_{i,k}$, compare the existing shortest distances with the total travel distances to each point, and set the smaller

values as the new shortest distances from $p_{1,m}$ to $p_{i+1,1}, p_{i+1,2}, p_{i+1,3}$, and $p_{i+1,4}$.

With this process, we have the shortest distances and their corresponding paths (a total of 16) from the starting points $p_{1,1}, p_{1,2}, p_{1,3}, p_{1,4}$ to the endpoints $p_{n,1}, p_{n,2}, p_{n,3}, p_{n,4}$. Then, the path with the shortest distance among them is determined as the desired path.

If each point on the trajectory has d possible configurations, the number of vertices in the graph for one starting point is $1 + (n - 1)d$, and the number of edges is $d + (n - 2)d^2$. For a graph with V vertices and E edges, the computational complexity of calculating the distances between each vertex is estimated to be $O(E)$. The current implementation of Dijkstra's algorithm uses binary heaps [20], whose computational complexity is $O(\log V)$. Thus, the complexity of Dijkstra's algorithm is estimated to be $O((V + E) \log V)$, and the complexity of this path-planning method for one starting point is estimated by

$$O(E) + O((V + E) \log V) = O(E + (V + E) \log V). \quad (13)$$

Since $V = 1 + (n - 1)d$ and $E = d + (n - 2)d^2$, the complexity of this method is estimated as

$$\begin{aligned} &O(E + (V + E) \log V) \\ &= O(d + (n - 2)d^2 + (1 + nd + (n - 2)d^2) \log(1 + (n - 1)d)) \\ &= O(nd^2 \log(nd)). \end{aligned}$$

4.3 Implementation and computational results

This section describes the implementation and experimental results of the proposed methods. The implementation of each procedure was based on an implementation [21] in the Python programming language.

For the path used in the experiment, we used the path generated by spline interpolation in Tests from 1 to 5 in Section 3.4. In the experiment, let $T = n = 15$, and the number of solutions of the inverse kinematic problem was 4 ($d = 4$) from the start to the end of the path. The computing environment is as follows: Host environment: Intel Core i7-1165G7, RAM 16 GB, Windows 11 Home, VMware Workstation 16 Player, Guest environment: RAM 13.2 GB, Ubuntu 22.04.3 LTS, Python: 3.10.12.

Tables 3 and 4 show the results of the experiment. The columns "Section 4.1" and "Section 4.2" show the results of the two methods proposed in each section. Table 3 shows the sum of the movements of the joints for each test. The result shows that the total change in the joint configuration obtained by the procedure in Section 4.2 (with Dijkstra's algorithm) is, on average, smaller than that obtained by the procedure in Section 4.1. Table 4 shows the computation time for each test. The average computation time due to the method in Sections 4.1 and 4.2 is the order of 10^{-4} [s] and 10^{-3} [s], respectively, which seems to be a practical computing time for both methods, although the method in Section 4.2 is slightly slower than the method in Section 4.1.

Table 3 The sum of the movements of the joints.

Test	Section 4.1 [rad]	Section 4.2 [rad]
1	8.3142	4.4013
2	11.5985	9.8986
3	15.0005	13.6731
4	8.5828	6.3277
5	7.1897	5.7108
Average	10.1371	8.0023

Table 4 Computing time of the optimal path calculations.

Test	Section 4.1 [10^{-4} s]	Section 4.2 [10^{-4} s]
1	1.96	39.4
2	2.16	42.8
3	2.90	33.0
4	2.90	40.1
5	4.44	36.4
Average	2.87	31.3

5 Concluding remarks

In this paper, we proposed an advanced method for solving the inverse kinematics and optimal path and trajectory planning problems for robot manipulators using spline curves and real quantifier elimination based on Comprehensive Gröbner Systems (CGS). The proposed method extends previous work by incorporating cubic spline interpolation for smooth path generation and optimizing joint configurations using shortest path algorithms.

The experimental results demonstrated that the proposed method can efficiently generate smooth trajectories and optimize joint configurations. The computation times for optimal path selection seem practical for real-time applications. The results also showed that the method based on Dijkstra’s algorithm for minimizing the sum of joint variations outperformed the method based on minimizing joint variations between each point.

Future work includes the following. For generating smooth paths, our experiments have shown that the spline interpolation method may not always generate feasible paths. Therefore, it is necessary to develop methods to ensure that the entire path fits within the feasible region. (We have already started working on this issue by the use of Bézier curves [22].) In calculating the optimal path, we assumed that the number of solutions of the inverse kinematics problem is the same at each point on the path. However, in practice, the number of solutions may vary depending on the point or the affine variety of the ideals defined by the inverse kinematic equations. Thus, investigation will be necessary for determination of the number and continuity of solutions to the inverse kinematics problem (such as detecting singular points).

Furthermore, the proposed method can be applied to other robot manipulators with different degrees of freedom and constraints, and the computational results can be compared with existing methods.

Acknowledgments

This work was partially supported by JKA and its promotion funds from KEIRIN RACE.

References

- [1] Siciliano, B., Khatib, O.: Springer Handbook of Robotics, 2nd edn. Springer, Berlin, Heidelberg (2016). <https://doi.org/10.1007/978-3-319-32552-1>
- [2] Faugère, J.-C., Merlet, J.-P., Rouillier, F.: On solving the direct kinematics problem for parallel robots. Research Report RR-5923, INRIA (2006). <https://hal.inria.fr/inria-00072366>
- [3] Kalker-Kalkman, C.M.: An implementation of Buchbergers' algorithm with applications to robotics. Mech. Mach. Theory **28**(4), 523–537 (1993) [https://doi.org/10.1016/0094-114X\(93\)90033-R](https://doi.org/10.1016/0094-114X(93)90033-R)
- [4] Silva, S., Schnitman, L., Cesca Filho, V.: A Solution of the Inverse Kinematics Problem for a 7-Degrees-of-Freedom Serial Redundant Manipulator Using Gröbner Bases Theory. Mathematical Problems in Engineering **2021**, 6680687 (2021) <https://doi.org/10.1155/2021/6680687>
- [5] Uchida, T., McPhee, J.: Triangularizing kinematic constraint equations using Gröbner bases for real-time dynamic simulation. Multibody System Dynamics **25**, 335–356 (2011) <https://doi.org/10.1007/s11044-010-9241-8>
- [6] Uchida, T., McPhee, J.: Using Gröbner bases to generate efficient kinematic solutions for the dynamic simulation of multi-loop mechanisms. Mech. Mach. Theory **52**, 144–157 (2012) <https://doi.org/10.1016/j.mechmachtheory.2012.01.015>
- [7] Horigome, N., Terui, A., Mikawa, M.: A Design and an Implementation of an Inverse Kinematics Computation in Robotics Using Gröbner Bases. In: Bigatti, A.M., Cayette, J., Davenport, J.H., Joswig, M., Wolff, T. (eds.) Mathematical Software – ICMS 2020, pp. 3–13. Springer, Cham (2020). https://doi.org/10.1007/978-3-030-52200-1_1
- [8] Otaki, S., Terui, A., Mikawa, M.: A Design and an Implementation of an Inverse Kinematics Computation in Robotics Using Real Quantifier Elimination based on Comprehensive Gröbner Systems. Preprint. arXiv:2111.00384 (2021). <https://doi.org/10.48550/arXiv.2111.00384>
- [9] Yoshizawa, M., Terui, A., Mikawa, M.: Inverse Kinematics and Path Planning of Manipulator Using Real Quantifier Elimination Based on Comprehensive Gröbner Systems. In: Computer Algebra in Scientific Computing. CASC 2023. Lecture Notes in Computer Science, vol. 14139, pp. 393–419. Springer, Cham (2023). https://doi.org/10.1007/978-3-031-41724-5_21

- [10] Weispfenning, V.: Comprehensive Gröbner Bases. *J. Symbolic Comput.* **14**(1), 1–29 (1992) [https://doi.org/10.1016/0747-7171\(92\)90023-W](https://doi.org/10.1016/0747-7171(92)90023-W)
- [11] Fukasaku, R., Iwane, H., Sato, Y.: Real Quantifier Elimination by Computation of Comprehensive Gröbner Systems. In: *Proceedings of the 2015 ACM on International Symposium on Symbolic and Algebraic Computation. ISSAC '15*, pp. 173–180. Association for Computing Machinery, New York, NY, USA (2015). <https://doi.org/10.1145/2755996.2756646>
- [12] Elephant Robotics Co., Ltd.: myCobot 280 M5 2023. (Accessed 2024-05-04) (2023). <https://www.elephantrobotics.com/mycobot-280-m5-2023>
- [13] Farin, G.: *Curves and Surfaces for CAGD: A Practical Guide*, 5th edn. The Morgan Kaufmann Series in Computer Graphics. Morgan Kaufmann, San Francisco, CA, USA (2002). <https://doi.org/10.1016/B978-1-55860-737-8.X5000-5>
- [14] Lynch, K.M., Park, F.C.: *Modern Robotics: Mechanics, Planning, and Control*. Cambridge University Press, Cambridge (2017)
- [15] Noro, M., Takeshima, T.: Risa/asir—a computer algebra system. In: *Papers from the International Symposium on Symbolic and Algebraic Computation. ISSAC '92*, pp. 387–396. Association for Computing Machinery, New York, NY, USA (1992). <https://doi.org/10.1145/143242.143362>
- [16] Kapur, D., Sun, Y., Wang, D.: A new algorithm for computing comprehensive Gröbner systems. In: *Proceedings of the 2010 International Symposium on Symbolic and Algebraic Computation. ISSAC '10*, pp. 29–36. Association for Computing Machinery, New York, NY, USA (2010). <https://doi.org/10.1145/1837934.1837946>
- [17] Nabeshima, K.: CGS: a program for computing comprehensive Gröbner systems in a polynomial ring [computer software]. <https://www.rs.tus.ac.jp/~nabeshima/softwares.html> (Accessed 2024-05-04) (2018)
- [18] Wolfram Research, Inc.: *Mathematica*, Version 13.1 [computer software], Champaign, IL, USA. Accessed 2024-05-04 (2022). <https://www.wolfram.com/mathematica>
- [19] Dijkstra, E.W.: A note on two problems in connexion with graphs. *Numer. Math.* **1**, 269–271 (1959) <https://doi.org/10.1007/BF01386390>
- [20] Cormen, T.H., Leiserson, C.E., Rivest, R.L., Stein, C.: *Introduction to Algorithms*, Fourth Edition, 4th edn. The MIT Press, Cambridge, MA, USA (2022)
- [21] simonritchie: Compute the shortest path of a graph using Dijkstra method and Python (in Japanese). <https://qiita.com/simonritchie/items/216eae753fc393da52af> (Accessed: 2024-05-04) (2023). <https://qiita.com/>

[simonritchie/items/216eae753fc393da52af](https://simonritchie.github.io/items/216eae753fc393da52af)

- [22] Hatakeya, R., Terui, A., Mikawa, M.: Towards trajectory planning of a robot manipulator with computer algebra using Bézier curves for obstacle avoidance. In: Nabeshima, K., Watt, S.M. (eds.) Proceedings of 10th International Symposium on Symbolic Computation in Software Science — Work in Progress Workshop. CEUR Workshop Proceedings, vol. 3754, pp. 21–27. RWTH Aachen University, Aachen, Germany (2024). <https://ceur-ws.org/Vol-3754/>